Characterisation of the atmosphere of WASP-76b using SPIRou

Thea Hood, Florian Debras, Claire Moutou, Baptiste Klein, Pascal Tremblin, Vivien Parmentier, Andres Carmona, Annabella Meech, Olivia Vénot, Adrien Masson, Pascal Petit, Sandrine Vinatier, Eder Martioli, Flavien Kiefer, Martin Turbet, and the ATMOSPHERIX consortium

Context

High-resolution observations (R ≥ 25000) performed by ground-based instruments are complementary to those from space. Indeed, by observing individual spectral lines, we can for example detect Doppler shifts due to dynamics. However, the data requires a complex analysis chain to extract the atmospheric signal, with it being buried in noise.

WASP-76b

- Ultra-hot Jupiter (**T_{eq} ≈ 2200K**)
- **Asymmetry** of Fe detected in limbs [2][3]
- Observed with SPIRou in transmission

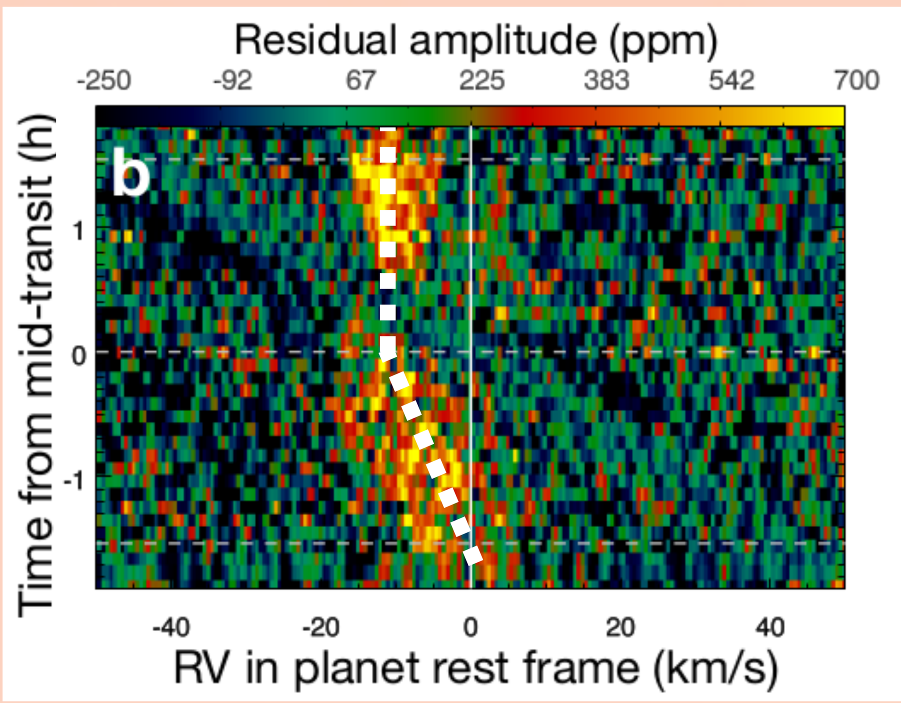

Figure 2: Detection of iron [2]

SPIRou [1]

- Located at the Canada-France Hawaii Telescope (CFHT)
- High-resolution observations (**R≈70 000**)
- Continuous coverage in near-infrared from **0.95 to 2.5 µm**
- **Transmission**/Emission spectroscopy

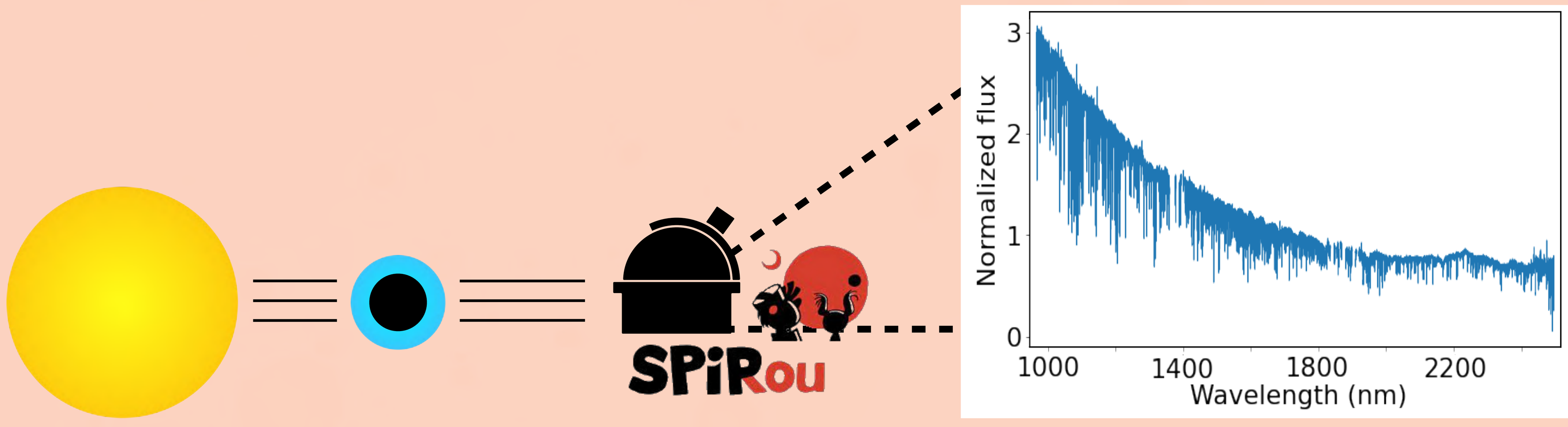

Figure 1: Representation of observation of WASP-76b in transmission and resulting spectral data from SPIRou used for study

Models

- 1D atmospheric models created using petitRADTRANS [4][5]
  - Isothermal profile
  - Solar H/He ratio
  - Molecules: **H_2O, CO, OH, HCN, C_2H_2**
- Broadened to account for rotation, winds and instrumental effects

Results: Detection of H_2O and CO

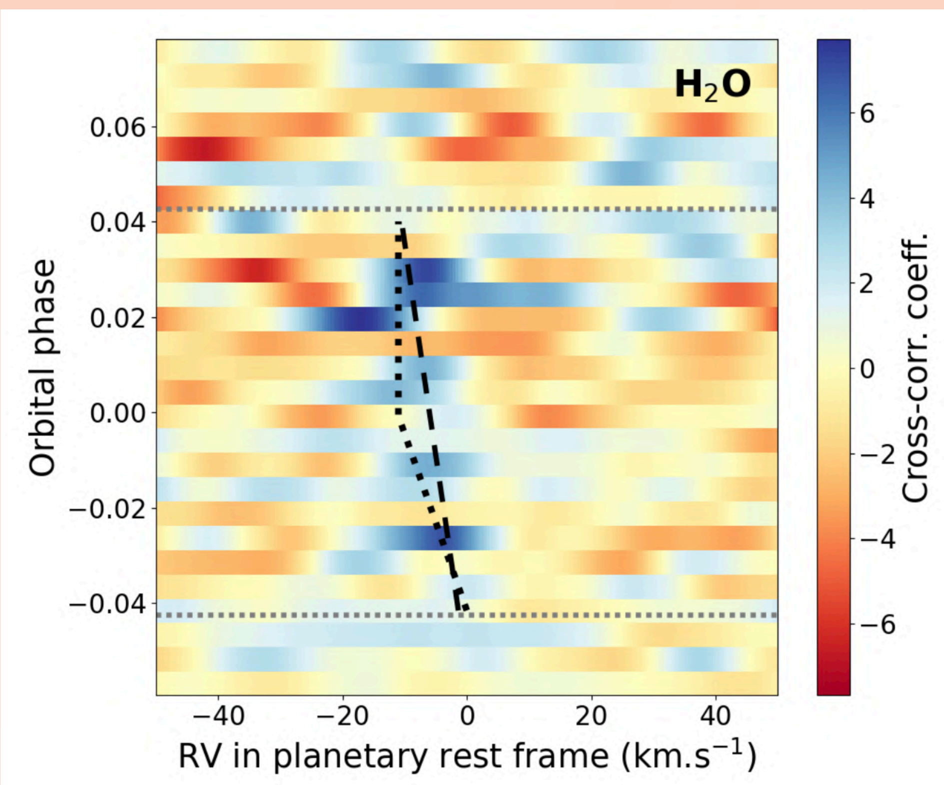

Figure 3: Combined CC grid with visible WASP-76b trace compared to Ehrenreich WASP-76b signature trace (red dotted line)

- Data reduced with **ATMOSPHERIX code [6]**
- Cross-correlation (CC) between reduced data and models to create maps
  - **Confirmed detection** of WASP-76b atmosphere
- Nested Sampling (NS) algorithm [7]
  - Estimation of H_2O and CO abundances
  - Upper limits inferred for OH, C_2H_2 and HCN

	Abundance estimate in $\log_{10}$(VMR)
H2O	-5.60 ± 0.21
CO	-4.46 ± 0.83
OH	< -4.86
HCN	< -7.05
C_2H_2	< -5.06

Table 1: Estimates of the abundances or their upper limits per molecule

Estimating C/O ratio and metallicity

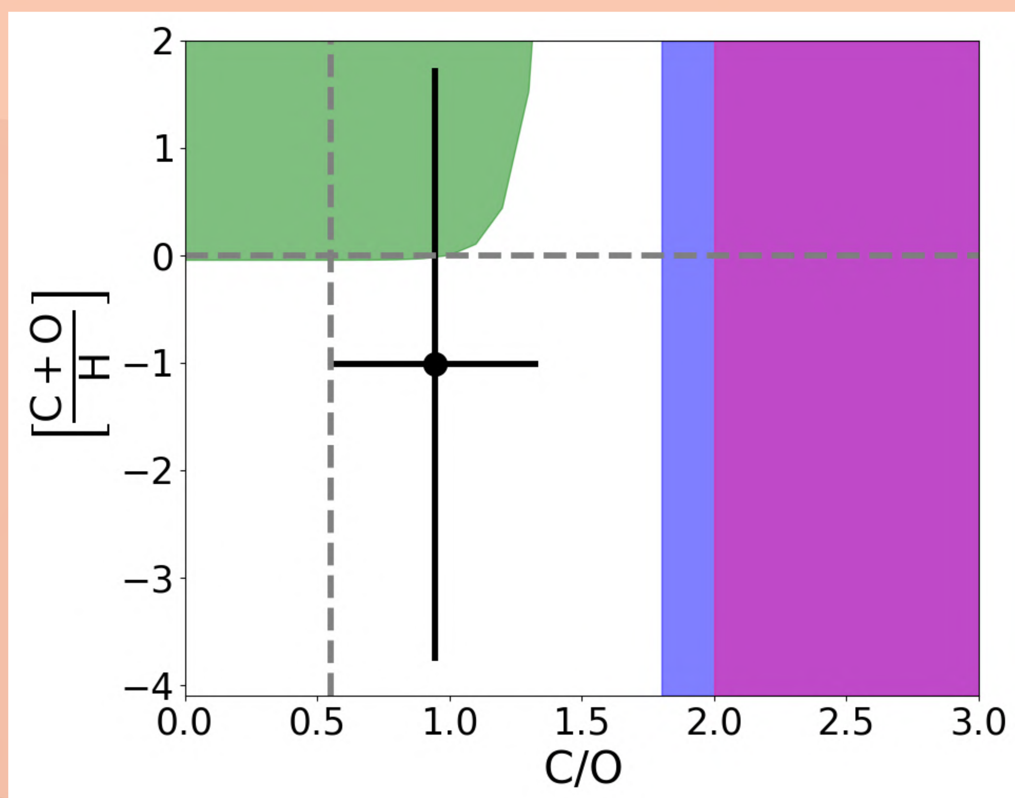

Figure 5: Representation of the estimated C/O and metallicity (with 2σ error bars), and areas of values excluded by the non-detections of OH (green), C_2H_2 (blue), and HCN (purple)

- Cautious estimation **C/O ~ 0.94** (≈ 1.7 x solar)
- Limits estimated for C/O and metallicity using ATMO forward models and upper limits of non-detected species

➡ **Greater constraints on C/O and metallicity required to place constraints on planet history**

Comparing to GCMs

- CO measured Doppler shift compatible with **temperature asymmetry between limbs**
- H_2O results compatible with **morning side optically thick clouds**

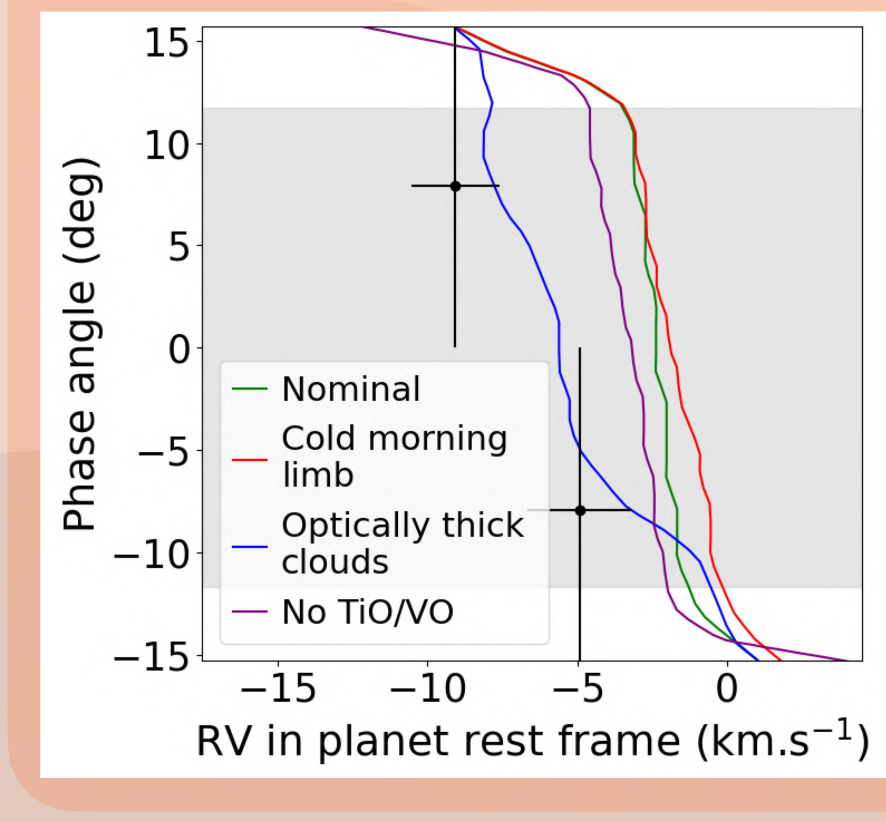

Figure 6: RVs obtained from the mean cross-correlation functions for each half of transit for H_2O (black) compared to GCM results from [8]

Hood et al., 2024

ATMOSPHERIX pipeline

References [1] Donati J. F., et al., 2020, MNRAS, 498, 5684, [2] Ehrenreich D., et al., 2020, Nature, 580, 597, [3] Kesseli A. Y., Snellen I. A. G., 2021, ApJ, 908, L17, [4] Mollière P., et al., 2019, A&A, 627, A67, [5] Mollière P., et al., 2020, A&A, 640, A131, [6] Klein, B., et al. 2024, MNRAS, 527, 544 [7] Buchner J., et al., 2014, A&A, 564, A125, [8] Wardenier, J. P., et al. 2023, MNRAS, 525, 4942